

Summer 7-12-2018

Synchronization in an externally driven mechanical oscillators experiment

Sumit Chhabria

Follow this and additional works at: https://digitalrepository.unm.edu/ece_etds



Part of the [Electrical and Computer Engineering Commons](#)

Recommended Citation

Chhabria, Sumit. "Synchronization in an externally driven mechanical oscillators experiment." (2018).
https://digitalrepository.unm.edu/ece_etds/415

This Thesis is brought to you for free and open access by the Engineering ETDs at UNM Digital Repository. It has been accepted for inclusion in Electrical and Computer Engineering ETDs by an authorized administrator of UNM Digital Repository. For more information, please contact disc@unm.edu.

Sumit Chhabria

Candidate

Electrical & Computer Engineering

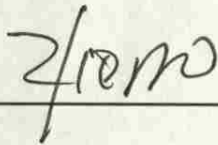
Department

This dissertation is approved, and it is acceptable in quality and form for publication:

Approved by the Thesis Committee:



Dr. Francesco Sorrentino, Chair



Dr. Rafael Fierro, Co-Chair



Dr. John Russell, Member

Synchronization in an externally driven mechanical oscillators experiment

by

SUMIT CHHABRIA

B.Tech, Electrical Engineering,
Pandit Deendayal Petroleum University, 2015

THESIS

Submitted in Partial Fulfillment of the
Requirements for the Degree of

Master of Science,
Electrical Engineering

The University of New Mexico

Albuquerque, New Mexico

July, 2018

Dedication

*To my parents, Harshita and Devendra Chhabria, and my sister Eshita Chhabria
who have always been a constant source of support and encouragement during my
graduate school.*

Acknowledgments

I would like to express my gratitude to my advisor, Dr Francesco Sorrentino for his useful comments, remarks and engagement through the learning process of this thesis. His office doors were always open whenever I ran into a trouble spot or had any question about my research and writing.

I would also like to thank my committee members Dr. Rafael Fierro and Dr. John Russell for providing me support on the way and valuable feedback for my work.

I would also like to acknowledge my collaborators for this work Dr. Karen Blaha and Dr. Fabio Della Rossa for their valuable inputs and comments towards this thesis. Further, I would like to mention my lab colleagues Afroza Shirin, Isaac Samuel Klickstein, Abu Bakar Siddique and Nicholas Torres for offering their help throughout my research and giving regular feedbacks for my work.

Finally, I want to express my very profound gratitude towards my parents (Harshita and Devendra Chhabria) for providing me with unfailing support and continuous encouragement throughout my years of study. This accomplishment would not have been possible without them. Thank you.

Synchronization in an externally driven mechanical oscillators experiment

by

SUMIT CHHABRIA

B.Tech, Electrical Engineering,
Pandit Deendayal Petroleum University, 2015

M.S., Electrical Engineering, University of New Mexico, 2018

Abstract

Our experimental system studies the effects of external controlled oscillation on directly and indirectly driven system of metronomes. This is analogous to many practical systems such as pacemaker effect on heart cells [14], external light effect on suprachiasmatic nucleus in the brain [21]. Here the pacemaker can be compared to external driving force to system where the heart cells are our oscillating system. Also in the suprachiasmatic nucleus cell system the external input is external light which synchronizes the cell. We explore the synchronization of directly and indirectly driven metronomes due externally provided forcing.

We designed an experimental setup to closely replicate the experimental system constructed by Martens et al[12]. The system consists of 3 platforms which contain 4 metronomes each (Figure 2.2). Each metronome and platform have UV sensitive dots which shines in dark room with UV light over it. This allows us to analyze the metronome motion using the video analysis toolbox of matlab. Our video analysis

code can compute the phases of metronomes and platforms which help us to qualitatively examine the system. We drive our system via a servo motor which is connected to the middle platform with an arm designed to reduce friction. The servo motor has a built-in feedback mechanism and its input is controlled via a PID controller to give sinusoidal input to the platform.

We observe in our experiments that when the metronomes are directly driven and the driving frequency is within $\pm 3\%$ of metronomes frequency, the metronomes Kuramoto order is near unity i.e. the metronomes synchronize. We observe that when the driving frequency is similar to metronomes placed on indirect driven platform, metronomes on indirect driven platform synchronize. While at the same time if driving frequency is different then metronome on directly driven platform, metronomes on directly driven do not synchronize.

Our experiments show that in order for a pacemaker to synchronize the oscillating system, the frequency of input should be similar as systems one is seeking to synchronize. This suggests that for example if we want to synchronize certain cells of heart while not affecting other, the pacemaker input should match the target cells frequency.

Contents

List of Figures	x
List of Tables	xiv
1 Introduction	1
1.1 Introduction	1
1.2 Motivation	2
1.3 Methodology	2
2 Experimental Setup Design and Analysis	4
2.1 Setup for Experiments with undriven metronomes	4
2.2 Setup for experiments with external driving (Servo motor)	7
2.3 Video Analysis of Experiment	10
2.3.1 Extracting metronome position from video	10
2.3.2 Quantitative measurement of the system from position data	11

Contents

3	Identifying System Parameters	14
3.1	Introduction	14
3.2	Metronome Parameters calculated Numerically	15
3.3	Experimentally Identifying Model Parameter without forcing	17
3.3.1	Get the state variables $(\phi, \dot{\phi})$ from the experiment	17
3.3.2	Finding model parameters which best fits the trajectory	18
3.3.3	Identifying parameters for different frequencies	20
3.4	Finding forced system parameters	21
3.4.1	Parameter fitting for Forcing	22
3.4.2	Comparing fits	24
4	Experiments	27
4.1	Metronomes on platform directly driven by servo motor	27
4.1.1	Driver frequency equal to Metronome frequency	28
4.1.2	Driver frequency is different than Metronome frequency	31
4.1.3	Metronome frequency and driver frequency are varied while keeping amplitude constant	33
4.1.4	Synchronization in metronomes when non-sinusoidal driving force is applied	33
4.2	Metronomes on platform indirectly driven by servo indirectly	36
4.2.1	Driver frequency equal to Metronome frequency	36

Contents

4.2.2	Driver frequency is different then Metronome frequency	37
4.3	Metronomes on platform directly and indirectly driven simultaneously	39
5	Conclusion & Future work	42
5.1	Conclusion	42
5.2	Future work	43
	References	44

List of Figures

2.1	Experimental Setup.	5
2.2	Experiment Layout.	5
2.3	Metronome with uv dot.	6
2.4	Photo of experiment under UV light.	6
2.5	Forcing to middle platform	7
2.6	Quanser Servo DC Motor	8
2.7	CAD model of servo motor arm	8
2.8	Servo DC motor connection.	8
2.9	PID response of servo motor.	9
2.10	Raw data of X-centroid of 4 metronomes on a platform.	10
2.11	Raw data of Y-centroid of 4 metronomes on a platform.	10
2.12	Filtered X-centroid data of metronome	11
2.13	Frequency variation of metronome (Natural frequency set to 120BPM) with respect to time.	12
2.14	Phase of metronome vs Phase of platform.	12

List of Figures

2.15	Kuramoto order between metronomes.	13
3.1	Metronome Components [12]	15
3.2	Metronome With UV dot and ϕ	17
3.3	ϕ and $\dot{\phi}$ before transient	18
3.4	ϕ and $\dot{\phi}$ after transient	19
3.5	Averaged trajectory	19
3.6	State ϕ and $\dot{\phi}$ simulation	20
3.7	Time Series Simulation	20
3.8	Parameter A for the equation 3.1	21
3.9	Parameter ϕ_0 for the equation 3.1	21
3.10	Parameter μ for the equation 3.1	21
3.11	Quasi periodic behavior	22
3.12	Plot of Cost function vs Forcing parameter	24
3.13	Curve fitting of F1	25
3.14	Curve fitting of F2	25
3.15	Curve fitting of F3	26
4.1	Direct forcing applied on metronomes.	28
4.2	Kuramoto order at lower amplitude(0.2)	29
4.3	Phase plot at 0.2 amp forcing	29

List of Figures

4.4	Kuramoto order at Higher amplitude(0.3)	30
4.5	Phase plot at 0.3 amp forcing	30
4.6	Kuramoto order variation with change in amplitude	31
4.7	Kuramoto order at 0.2 amplitude and 132BPM forcing	31
4.8	Phase plot at 0.2 amp 132BPM forcing	32
4.9	Kuramoto order variation with change in driver frequency and amplitude	32
4.10	Kuramoto order variation with a change in the driver frequency and the metronome frequency	33
4.11	Driver square waveform with frequency different then metronomes .	34
4.12	Driver square waveform with frequency same as metronomes	34
4.13	Driver triangle waveform with frequency different then metronomes .	35
4.14	Driver triangle waveform with frequency same as metronomes	35
4.15	Indirect forcing applied on metronomes.	36
4.16	Order when forcing is indirect of 0.25 amplitude and 120BPM	37
4.17	Phase of metronome with respect to phase of Metronomes when forcing is indirect of 0.25 amplitude and 120BPM	37
4.18	Kuramoto order plot of indirectly driven metronomes with 0.2 Amplitude, 144BPM forcing	38
4.19	Phase plot of indirectly driven metronomes with 0.2 Amplitude, 144BPM forcing	38

List of Figures

4.20	Kuramoto order variation with the change in forcing amplitude and frequency.	39
4.21	Kuramoto order of directly and indirectly driven metronomes when driver frequency is same as metronomes on directly driven platform	40
4.22	Kuramoto order of directly and indirectly driven metronomes when driver frequency is same as metronomes on indirectly driven platform.	41

List of Tables

3.1	A and μ numerical values	16
3.2	Values from Physics vs Curve fitting values of parameters	24

Chapter 1

Introduction

1.1 Introduction

Synchronization in coupled oscillators was first observed by Christiaan Huygens who observed that two pendulum clocks suspended on a beam always exact anti-phase motion[6]. He explained this synchronization was due to vibration traveling across the beam. In 2002 Kuramoto showed that synchronous and disordered states could coexist[9]. Kuramoto work led to extensive Kuramoto's work led to extensive theoretical studies in order and disorder coexists in population [1], [11], [15].The experiment setup developed by Karen Blaha [3] studied the chimera states [2] arising in population of mechanical oscillators by varying the type of coupling between them.

We extended this experiment to study the effect of an external control action on directly and indirectly driven population of mechanical oscillators – metronomes. We developed external driving for metronomes on a platform via a servo motor. The layout of the experiment setup is discussed in chapter 2. In chapter 3 we find the parameters of our model by fitting experiment data to a model. In chapter 4 we discuss the experiments performed and results obtained.

1.2 Motivation

The external control action on population of oscillators is analogous to many practical systems such as a pacemaker acting on heart cells[14], and the effect of sunlight on the circadian rhythm via the suprachiasmatic nucleus in the brain[20]. In the heart, the external pacemaker drives a population of oscillating heart cells while in our system the servo drives a population of oscillating metronomes. In the suprachiasmatic nucleus the external input is external light which synchronizes cells in the brain.

We want to show the synchronization of directly and indirectly driven metronomes due to a certain externally provided forcing.

1.3 Methodology

We use external driven model given by Martens et al 2013[12]:

$$\underbrace{\ddot{\phi}(t)}_{\text{Term 1}} + \underbrace{\mu\dot{\phi}(t)\left(1 - \frac{\phi^2(t)}{\phi_0^2}\right)}_{\text{Term 2}} + \underbrace{A \sin \phi(t)}_{\text{Term 3}} + \underbrace{\frac{\omega^2}{\Omega} \cos \phi(t)\Phi(t)}_{\text{Term 4}} = 0 \quad (1.1)$$

$\phi(t)$ = Metronome angle, $\Phi(t)$ = Swing Angle

Ω = Swing frequency, ω = Metronome frequency.

Here our external control input through servo motor to the platform such that swing angle (Φ) = external input($F(t)$) (Figure2.2).

In Equation 1.1 term 1 is inertia, term 2 is non-linear damping, term 3 is force of restitution and term 4 is driving swing inertia.

To study the synchronization of oscillators we use the Kuramoto order parameter which is defined for the Kuramoto model [8]:

$$\frac{d\theta_i}{dt} = \omega_i + \frac{K}{N} \sum_{j=1}^N \sin(\theta_j - \theta_i), i = 1..N, \quad (1.2)$$

Chapter 1. Introduction

where the system is composed of N limit-cycle oscillators, with phase θ_i , natural frequency ω_i and coupling K .

The Kuramoto order parameter is given by:

$$r e^{i\psi} = \frac{1}{N} \sum_{j=1}^N e^{i\theta_j} \quad (1.3)$$

Here the magnitude (r) represents the phase-coherence of the population of oscillators and ψ indicates the average phase. When $r=1$, the oscillators are fully synchronized; when r is near 0, the oscillators are desynchronized. The Kuramoto model has been used to model beating of heart [14], flashing fireflies [4], pedestrians on a bridge [17], chemical oscillators [7] [18], metabolic oscillation in yeast cell [5] and life cycle of phytoplankton [13], circadian clocks in the brain [10], superconducting Josephson junction [19].

Chapter 2

Experimental Setup Design and Analysis

2.1 Setup for Experiments with undriven metronomes

We designed an experimental setup to closely replicate the experimental system constructed by Martens et al [12] (Figure 2.1). The system consists of 3 platform which can support up to 15 metronome each. These platforms are connected to the frame by bearing blocks, and coupled to each other by extension springs that are attached to the platform rod with adjustable coupling blocks (Figure 2.2). The distance between the bearing and platform is typically 22cm.

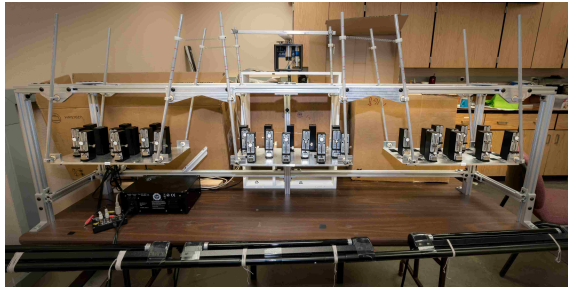


Figure 2.1: Experimental Setup.

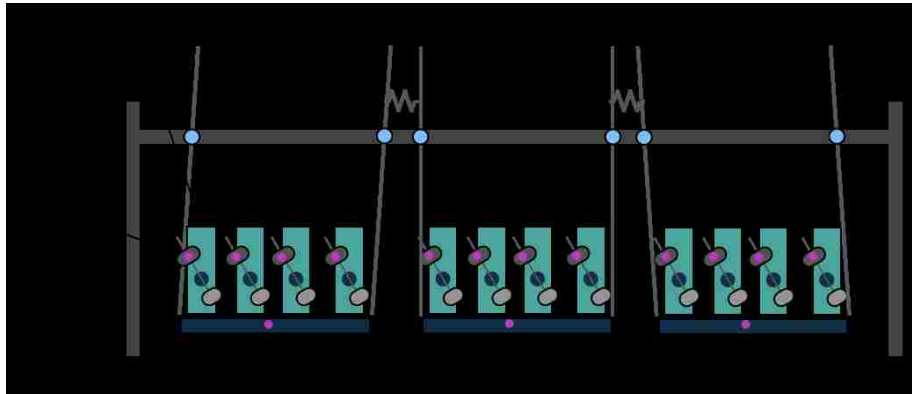


Figure 2.2: Experiment Layout.

To compare forcing inertia of system we compare the masses of metronomes to mass of the platform. The total mass of each metronome is 93g, the mass of the platform along with the rods and bearings is 615g. For experiments, we place 12 metronomes on each platform so the ratio of mass of metronomes to mass of platform is approximate 2:1 (Not all metronomes swing during experiment).

We place a UV sensitive dot at the top of the arm of each metronome and on each swing. We perform the experiments in a dark room lit with ultraviolet lights to make the dots fluoresce, see Figure 2.3. We record experiments with a Nikon D90 camera with a 18-55 mm Nikon DX lens recording at 60 frames per second(fps).

Chapter 2. Experimental Setup Design and Analysis

The swinging of the UV dots allows us to isolate the motion of the metronomes in post-processing of the video. (Figure 2.4).

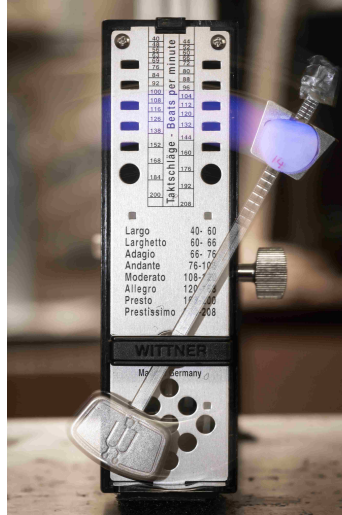


Figure 2.3: Metronome with uv dot.

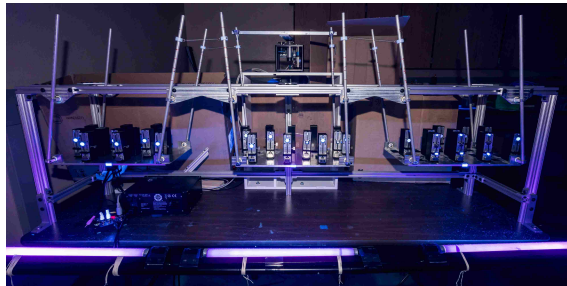


Figure 2.4: Photo of experiment under UV light.

We perform the experiments following a standardized protocol. The Bearing blocks are first set to the desired offset values and secured in place. We set the frequency on each metronome, wind them and place them on the platforms. The metronomes are placed to swing of the pendulums parallel to the platform's motion. The ends of the rod are connected by Extension springs in between. We then place

the camera and record the experiment under UV light.

2.2 Setup for experiments with external driving (Servo motor)

We use a Quanser Rotary Servo Base to give input to the system. It consists of a DC motor in an aluminum frame with built-in feedback mechanism with PID controller to give desired response from the motor (Figure 2.6). The Servo motor sits on a platform behind the frame so unintended motion doesn't transfer to the experimental system. The motor is connected to the middle platform via an arm; it directly forces the middle platform and indirectly forces the side platform via the coupling spring (Figure 2.5). The arm connecting the servo motor to the system was designed with CAD software (Figure 2.7) to have the least friction. The arm was 3d printed to give precision (Figure 2.8).

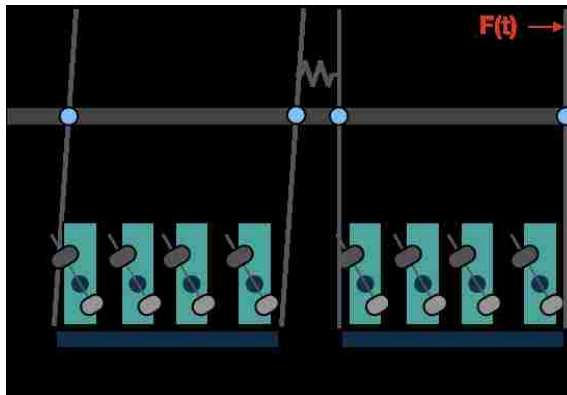


Figure 2.5: Forcing to middle platform

Chapter 2. Experimental Setup Design and Analysis

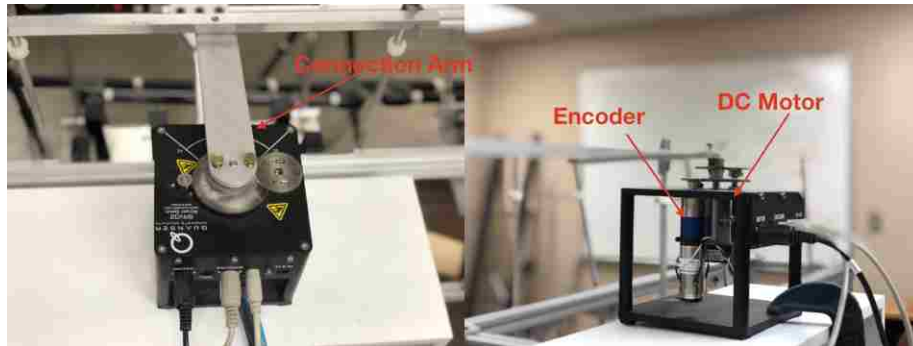


Figure 2.6: Quanser Servo DC Motor



Figure 2.7: CAD model of servo motor arm

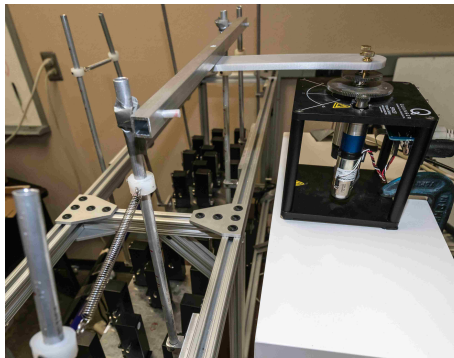


Figure 2.8: Servo DC motor connection.

Chapter 2. Experimental Setup Design and Analysis

The Servo motor gives sinusoidal input to the platform. The Quanser servo motor uses a PID controller. PID gains are modeled using first principal modeling. The frequency response of the servo motor and parameters are given by Quanser [16]. These gains are fine tuned to account for the weight of servo arm. The PID gain response is given by figure2.9.

$$u(t) = K_p e(t) + K_i \int_0^t e(t) + K_d \frac{de(t)}{dt} \quad (2.1)$$

The optimal gains are:

$$K_p = 30 \text{ V/rad}$$

$$K_d = 2 \text{ V.s/rad}$$

$$K_i = 0.157 \text{ V/(rad}\times\text{s)}$$

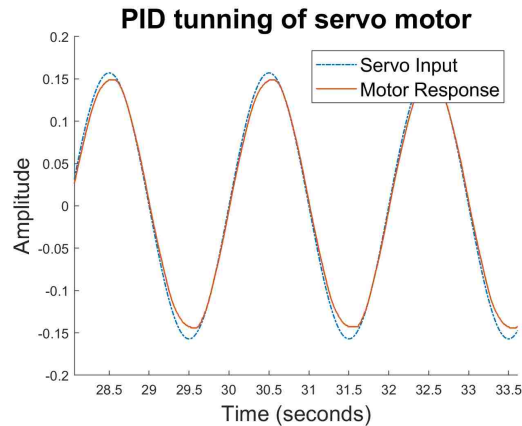


Figure 2.9: PID response of servo motor.

2.3 Video Analysis of Experiment

2.3.1 Extracting metronome position from video

We analyze the videos with the Matlab video analysis toolbox to measure the horizontal position (figure 2.10) and vertical position (figure 2.11) of the metronome and platform dots.

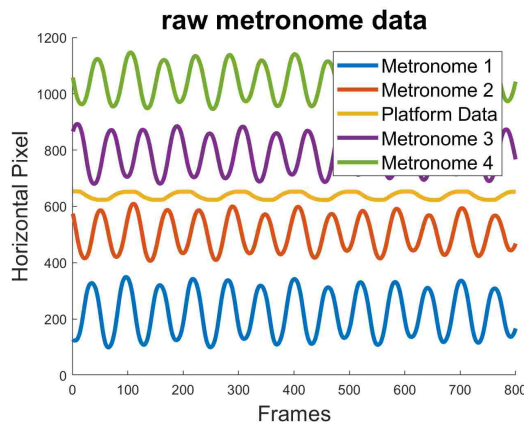


Figure 2.10: Raw data of X-centroid of 4 metronomes on a platform.

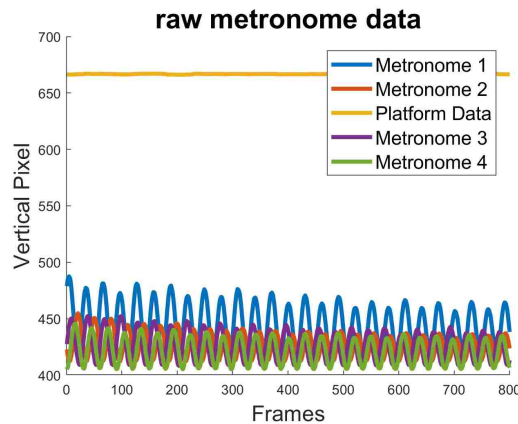


Figure 2.11: Raw data of Y-centroid of 4 metronomes on a platform.

We identify platform data whose vertical location is maximum in raw data (Figure 2.11). We filter the raw centroid data of metronome by removing the platform data from it.

2.3.2 Quantitative measurement of the system from position data

From position vs time plots (Figure 2.10) we extract peaks of data (Figure 2.12).

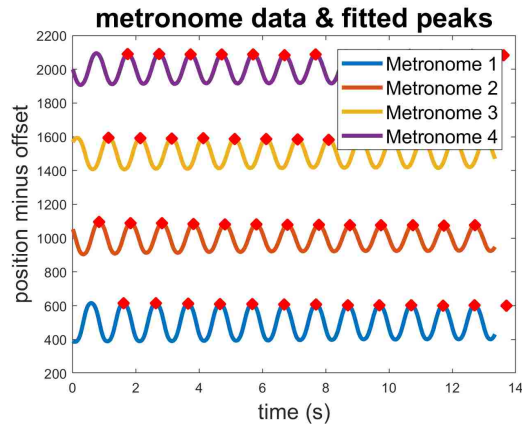


Figure 2.12: Filtered X-centroid data of metronome

We identify the peaks of the metronome oscillations which help us to look at frequency vs time (Figure 2.13) plot.

Chapter 2. Experimental Setup Design and Analysis

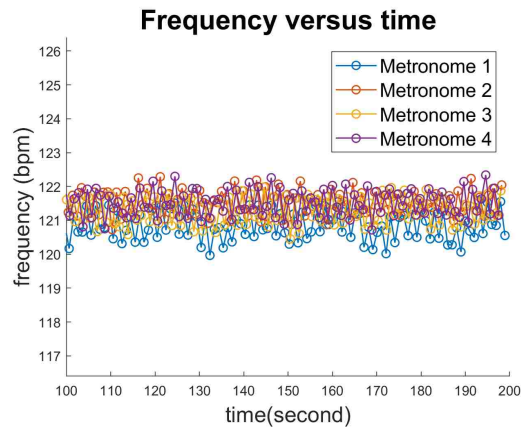


Figure 2.13: Frequency variation of metronome (Natural frequency set to 120BPM) with respect to time.

Using peak analysis, we compute the phase of each metronome and plot the phase of metronome vs phase of platform plots(Figure2.14).

Also we are able to compute the Kuramoto order (Equation 1.3) between metronomes(Figure 2.15).

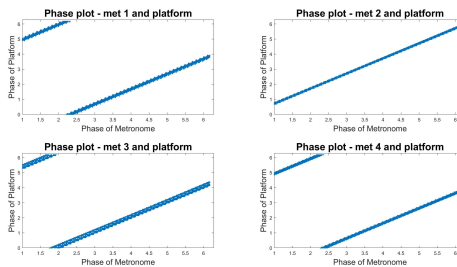


Figure 2.14: Phase of metronome vs Phase of platform.

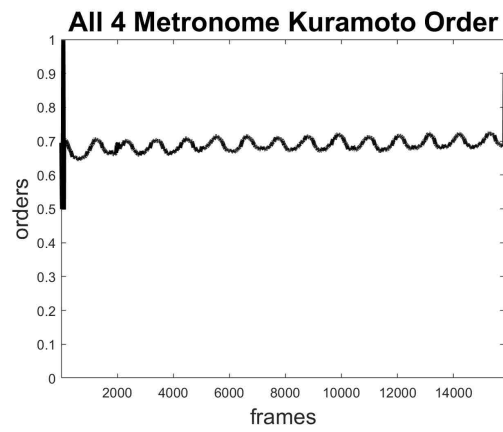


Figure 2.15: Kuramoto order between metronomes.

Chapter 3

Identifying System Parameters

3.1 Introduction

We want to compare the experiment to simulation using Martens model. To use this model, we have to fit parameters. We calculate Metronome parameters from physics equations of model(section 3.2). Then we compare these with our experiments parameters fitting without driving (section 3.3) and fitting with driving (section 3.4).

The dynamics of metronomes on a platform are (Martens et al 2013 [12]) :

$$\ddot{\phi} + \mu\dot{\phi}\left(1 - \frac{\phi^2}{\phi_0^2}\right) + A \sin \phi + \frac{\omega^2}{\Omega} \cos \phi \ddot{\Phi} = 0 \quad (3.1)$$

ϕ = Metronome angle, Φ = Swing Angle

Ω = Swing frequency, ω = Metronome frequency.

Here A corresponds to force of restitution of metronome and depends on frequency of metronome. ϕ_0 is half of standard displacement angle of an uncoupled, non-accelerated metronome pendulum mounted on a horizontal surface. μ is van der Pol

term to model the escapement mechanism. In section 3.3, we experimentally fit μ , ϕ_0 and A by experiments of metronome without driving. In section 3.4 we fit μ , ϕ_0 , A and forcing term with driving.

3.2 Metronome Parameters calculated Numerically

In this section fit parameters of our systems from equations from free body representations of the system. This helps us to verify our results from experiment curve fitting of the system and gives idea for initial guess in our curve fitting plots.

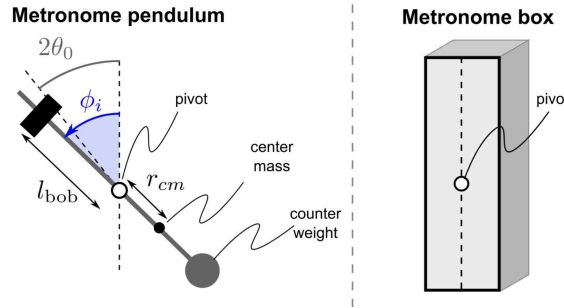


Figure 3.1: Metronome Components [12]

$$m_{bob} = 5.5g \text{ (Mass of bob)}$$

$$m_p = 22.6g \text{ (Mass of Pendulum)}$$

$$m = m_{bob} + m_p = 28.1g \text{ (Total mass of swinging part)}$$

From Martens paper[12] we have our system equation as:

$$\ddot{\phi} = -\frac{mgr_{cm}}{I} \sin \phi - \frac{\nu_m}{I} \dot{\phi} \left[\left(\frac{\dot{\phi}}{\phi_0} \right)^2 - 1 \right] - \frac{mr_{cm}}{I} L \cos \phi \ddot{\Phi} \quad (3.2)$$

Here the distance of the center of mass of the pendulum from the pivot point (the point at which the pendulum swings) is $r_{cm} = (m_0 l_0 + m_{bob} l_{bob})/m = r_0 +$

Chapter 3. Identifying System Parameters

$\frac{m_{bob}}{m}l_{bob}$. (Where l_{bob} is distance between the bob and pivot point).

For metronome at 208bpm, $l_{bob} = 26mm$, we balance it at edge of blade to find the center of mass to be at distance $r_{cm} = -7.5mm$, which gives $r_0 = -12.58mm$ which is a constant. Therefore, $r_{cm} = |-0.01258 + 0.1957.l_{bob}|$ where, $l_{bob} = 0.073 - 0.00022 \times f(bpm)$ ([12])

The second moment of inertia of pendulum is given by

$$I = m_0l_0^2 + m_{bob}l_{bob}^2$$

$$I = mgr_{cm}\omega^{-2},$$

$$I_0 = I|_{f=208} - m_{bob}l_{bob}^2 = 1.29 \times 10^{-5} \text{ which is a constant.}$$

$$I = 1.29 \times 10^{-5} + 5 \times 10^{-3}.l_{bob}^2$$

In equation 3.4 the forcing is introduced in terms of platform swing angle (Φ).

We give sinusoidal input to swing, $\Phi = C \sin(\omega_0 t)$.

$$\ddot{\Phi} = -C\omega^2 \sin(\omega_0 t)$$

$$\ddot{\Phi} = K\phi, \text{ where } K \text{ is constant}$$

Our systems equation is given by

$$\ddot{\phi} + \mu\dot{\phi}\left(\frac{\phi^2}{\phi_0^2} - 1\right) + A \sin \phi + \omega \cos \phi \theta = 0 \quad (3.3)$$

Here,

$$A = \frac{mgr_{cm}}{I} \quad \mu = \frac{\nu_m}{I} \quad K' = -\frac{mr_{cm}}{I}L * K \quad (3.4)$$

K' depends on forcing constant. Therefore its difficult to compute it numerically. A and μ are calculated numerically for different frequencies to be:

Frequency	A(Num)	μ (Num)
112	32.3156	0.0678
116	34.708	0.069
120	37.1747	0.0702
126	41.0172	0.0721

Table 3.1: A and μ numerical values

3.3 Experimentally Identifying Model Parameter without forcing

As first step we identify μ , ϕ_0 and A , using the undriven metronome. To do that we follow this strategy:

- Compute the state variables $(\phi, \dot{\phi})$ from the experiment
- Find the model parameters that best fit the trajectory

3.3.1 Get the state variables $(\phi, \dot{\phi})$ from the experiment

We perform a table top experiment with a single metronome set to 120BPM frequency. We get X and Y displacement of UV dot on metronome in term of pixels (Figure 3.2). We can compute ϕ from the UV dot dot (Figure 3.2). From the known frame rate we can get $\phi(t)$. We then compute $\dot{\phi}(t)$ using central difference.

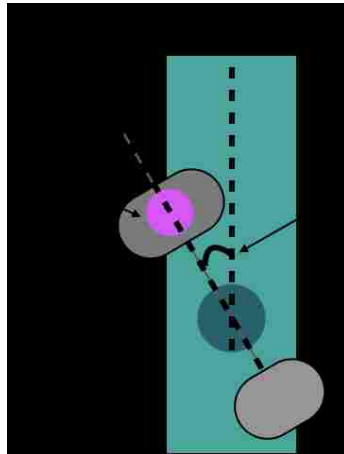


Figure 3.2: Metronome With UV dot and ϕ .

3.3.2 Finding model parameters which best fits the trajectory

To identify the model parameters (since the model is non-linear) we directly optimize (using Matlab `fminsearch` routine) the cost function

$$\int_0^{T^f} (\phi(t) - \phi^{exp}(t))^2 dt \quad (3.5)$$

where $\phi^{exp}(t)$ is the experiment data and $\phi(t)$ is the solution of the differential equation (3.1) (we set $\phi(0) = \phi^{exp}(0)$), up to a certain time T^f .

Since the system is periodic, we have chosen $T^f = nT$ (the oscillation period) in order to avoid local minima.

We plot $\phi^{exp}(t)$ vs $\dot{\phi}^{exp}(t)$ (figure 3.3). We remove the initial transient and observe the plot(figure 3.4) settles to a limit cycle.

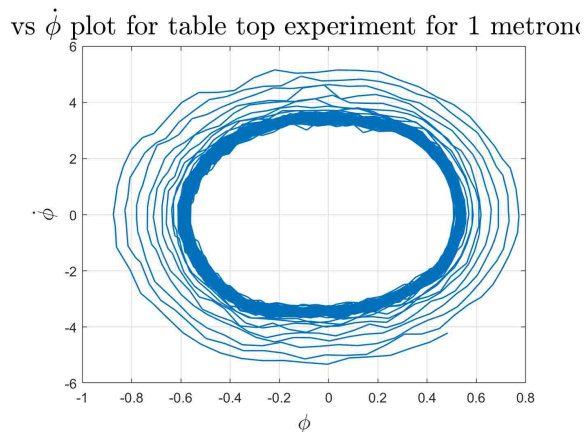


Figure 3.3: ϕ and $\dot{\phi}$ before transient

Chapter 3. Identifying System Parameters

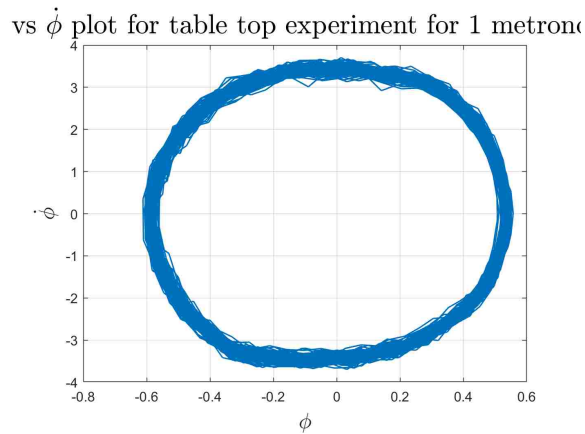


Figure 3.4: ϕ and $\dot{\phi}$ after transient

To get the asymptotic solution, we take average of the trajectories.

We find the points where $\phi(t)$ changes from negative to positive. At these points will be different time periods for single cycle on $\phi(t)$ vs $\dot{\phi}(t)$ plot. We average out to find average time period of metronome to complete one cycle. Now we sample all the cycles to the average time period and then find out the average of these trajectories (Figure 3.7) and use it to fit our model equation to find parameters.

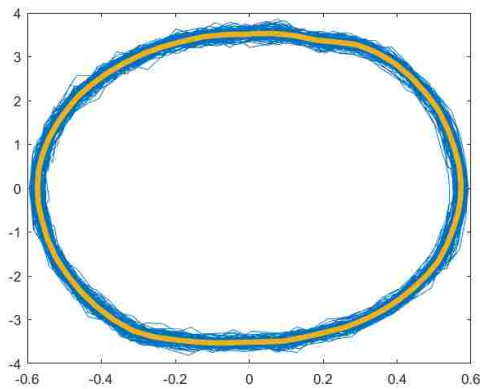


Figure 3.5: Averaged trajectory

Chapter 3. Identifying System Parameters

Once we find suitable parameter set we can refine the parameters identification making the trajectory longer and longer (two periods, three periods, etc...)

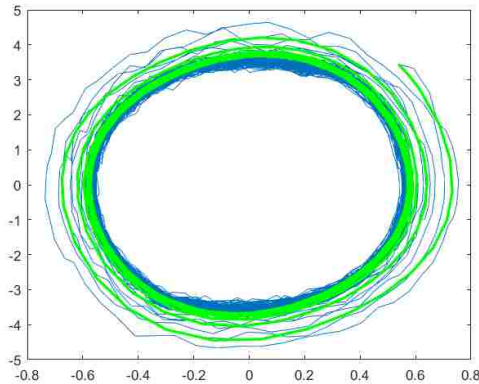


Figure 3.6: State ϕ and $\dot{\phi}$ simulation

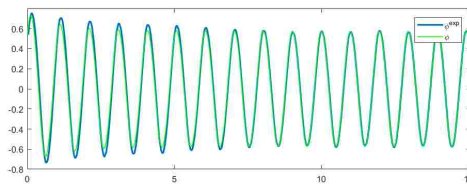


Figure 3.7: Time Series Simulation

The identified parameters for a single metronome on a platform with natural frequency 120BPM: $A = 42.2853$, $\mu = 0.6365$, $\phi_0 = 0.286$.

3.3.3 Identifying parameters for different frequencies

We want to check now how these parameters changes with change in frequency of metronome. Similar experiments were conducted for 108 BPM, 112 BPM, 116 BPM, 120 BPM, 126 BPM, 132 BPM.

Chapter 3. Identifying System Parameters

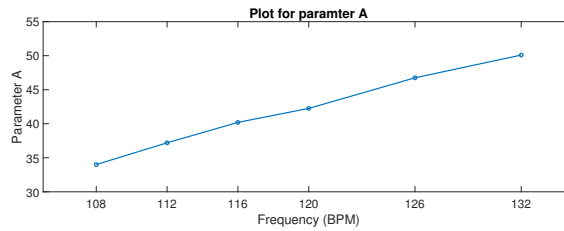


Figure 3.8: Parameter A for the equation 3.1

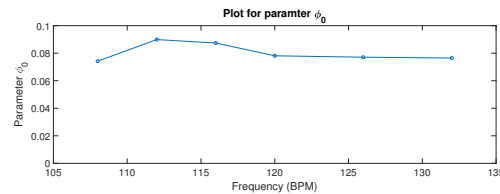


Figure 3.9: Parameter ϕ_0 for the equation 3.1

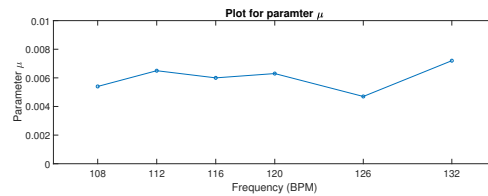


Figure 3.10: Parameter μ for the equation 3.1

We can see from figure 3.8 that parameter A changes linearly while parameter ϕ_0 and μ remains constant (figure 3.9 & 3.10). This can be seen in equation 3.4 that parameter A depends on length of bob (which is directly proportional to frequency) while parameter ϕ_0 and μ are property of metronome (Section 3.1).

3.4 Finding forced system parameters

We identify the system parameters with forcing. We want to identify K' in equation 3.3. ■

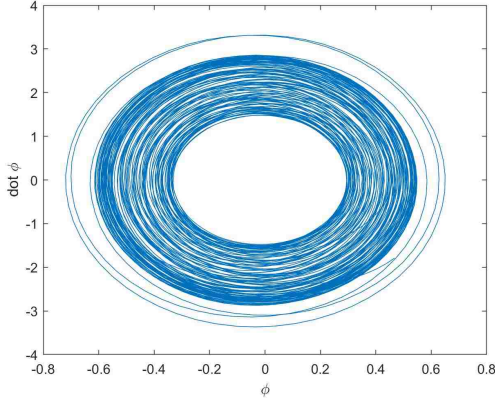


Figure 3.11: Quasi periodic behavior

In the previous case we had a limit cycle, but here we get a quasi periodic behavior(as seen in figure 3.11)

3.4.1 Parameter fitting for Forcing

We tried fitting the forcing parameter with the model but we always got stuck in local minimum as we didn't get good initial guess. We take the model in terms of l_{bob} as we expand martens equation.

Our model equations are given by:

$$\ddot{\phi} = -\frac{mgr_{cm}}{I} \sin \phi - \frac{\nu_m}{I} \dot{\phi} \left[\left(\frac{\phi}{\theta_0} \right)^2 - 1 \right] - \frac{mr_{cm}}{I} L \cos \phi \ddot{\theta} \quad (3.6)$$

Which can be written as:

$$\ddot{\phi} = -A \frac{(b_0 + b_1 * l_{bob})}{(a_0 + a_1 * l_{bob}^2)} \sin \phi - \frac{\nu_m}{(a_0 + a_1 * l_{bob}^2)} \dot{\phi} \left[\left(\frac{\phi}{\theta_0} \right)^2 - 1 \right] - F \frac{(b_0 + b_1 * l_{bob})}{(a_0 + a_1 * l_{bob}^2)} \cos \phi \ddot{\theta} \quad (3.7)$$

where, $A = m * g$ and $F = m * L * forcing$

Expected Values of parameters:

Chapter 3. Identifying System Parameters

$a_0 = 1.29 * 10^{-5}$, $a_1 = 5 * 10^{-3}$, $b_0 = -0.01258$, $b_1 = 0.1957$, $A = 0.2744$, θ_0 , μ_m and F are property of metronome and forcing.

For fitting we looked in to experiment where the metronome frequency was fixed to 120BPM, and the forcing frequency was changed. In Martens equation only forcing term should change for all the experiment.

We performed 3 experiments on 120BPM metronome:

F1: Amplitude 0.2, Frequency 0.6 hz

F2: Amplitude 0.2, Frequency 0.8 hz

F3: Amplitude 0.2, Frequency 1.2 hz

We are trying to fit a_0 , a_1 , b_0 , b_1 , A , μ_m , θ_0 , F_1 , F_2 , F_3 .

Here F_1 , F_2 , F_3 are forcing term in different experiment.

Since we are fitting 11 parameters, choosing initial guess for curve fitting is very important.

To start fitting, I fixed first a_0, a_1, b_0, b_1 from our physics calculation of model. Then to find the A , μ_m , θ_0 , I ran the curve fitting code for small duration for one of the forcing and tried different initial condition so as the fitting is good. Once I had A , μ_m , θ_0 , I had to only fit F_1 , F_2 , F_3 . For this I found the cost function plot vs the forcing parameter (figure 3.12) so that I am not stuck in local minimum for each forcing term.

Chapter 3. Identifying System Parameters

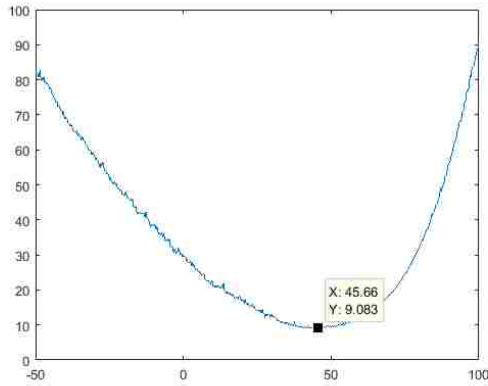


Figure 3.12: Plot of Cost function vs Forcing parameter

3.4.2 Comparing fits

Parameter	Values from Physics	Curve fitting Value	error
a_0	$1.29 * 10^{-5}$	$1.29 * 10^{-5}$	0
a_1	$5 * 10^{-3}$	$5 * 10^{-3}$	0
b_0	-0.01258	-0.01258	0
b_1	0.1957	0.1957	0
A	0.2744	0.29106	0.0166
μ_m	—	$2.042 * 10^{-5}$	—
θ_0	—	0.2724	—
$F1$	—	12.6795	—
$F2$	—	11.0965	—
$F3$	—	44.9978	—

Table 3.2: Values from Physics vs Curve fitting values of parameters

- a_0, a_1, b_0, b_1 were fixed while curve fitting.
- A is negative cause we have taken $r_c m$ to be negative.

Chapter 3. Identifying System Parameters

- θ_0 comes to be 16degree. In martens paper they have mentioned it to be 17-18 degree.
- Curve fitting of F1, F2 and F3 can be seen in figure3.13, 3.14, 3.15.

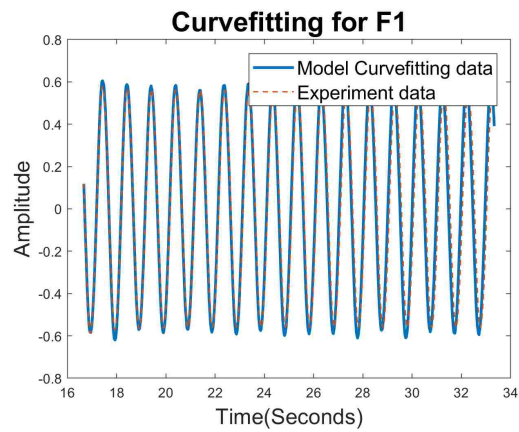


Figure 3.13: Curve fitting of F1

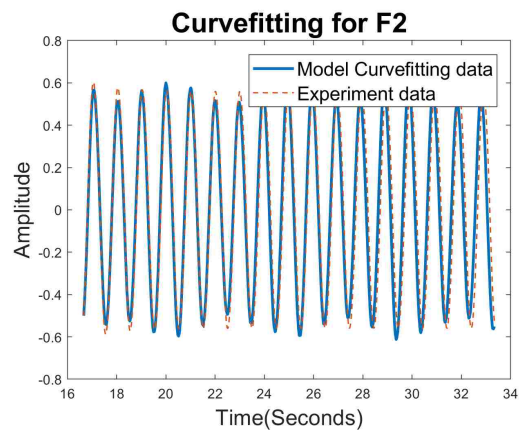


Figure 3.14: Curve fitting of F2

Chapter 3. Identifying System Parameters

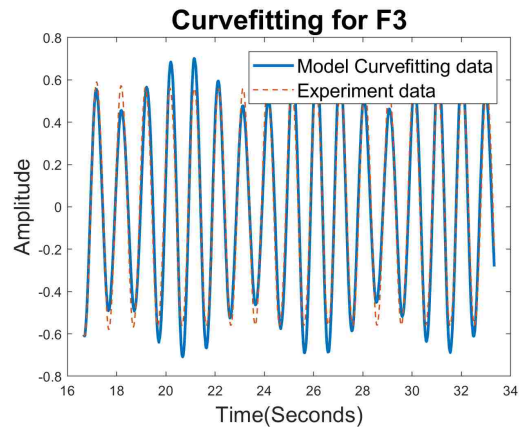


Figure 3.15: Curve fitting of F3

Chapter 4

Experiments

4.1 Metronomes on platform directly driven by servo motor

Four metronomes are placed on a platform which is directly driven by a servo motor (Figure 4.1). The metronome frequency is fixed to 120BPM, forcing is applied through a servo motor attached to the middle platform. The forcing signal of a sinusoidal wave is applied and we change its amplitude and frequency.

We compute the Kuramoto order [9](Section 1.3) between these four metronome to check the synchronization between them. If the Kuramoto order is near one, we say metronomes are synchronized with each other.

We also make a phase plot of the metronome against the phase of the platform. If there is a locking between the phase of metronome and platform we see the straight lines with some slope on the x-axis.

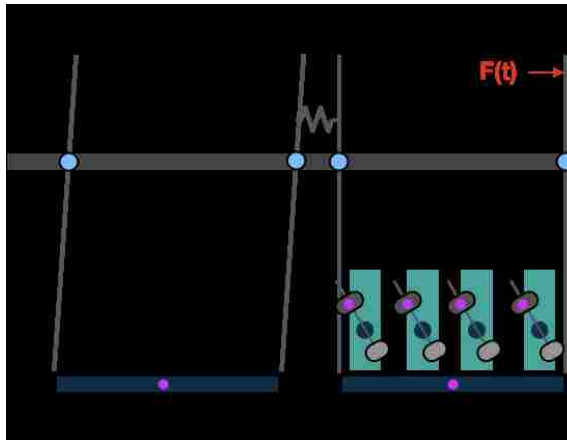


Figure 4.1: Direct forcing applied on metronomes.

4.1.1 Driver frequency equal to Metronome frequency

Four metronomes (set to 120BPM) are placed on a platform and driven by a servo motor (Figure 4.1). We fix the forcing frequency to 120BPM and change the amplitude of the sinusoidal wave.

When lower amplitude (0.2 amplitude) of forcing is applied, not all metronomes synchronize with each other and the Kuramoto order is less than 1 (Figure 4.2). We also see this in a phase plot between the phase of metronome and the phase of platform (Figure 4.3). We see that the phase of metronomes 2, 3 and 4 locks directly proportional to the phase of the platform while phase of metronome 1 is π anti-phase with the phase of platform.

Chapter 4. Experiments

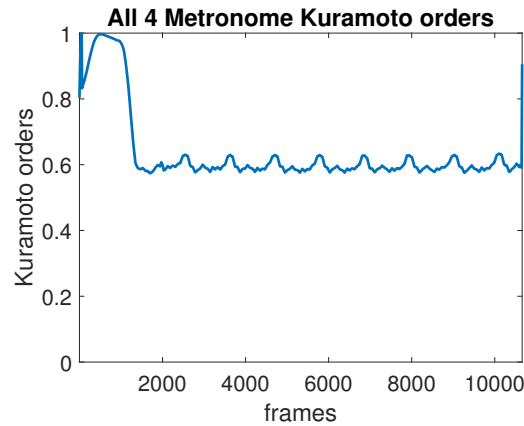


Figure 4.2: Kuramoto order at lower amplitude(0.2)

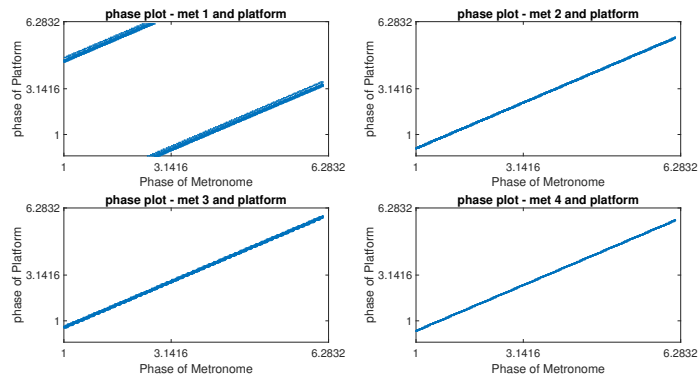


Figure 4.3: Phase plot at 0.2 amp forcing

When higher amplitude (0.3 amplitude) of the forcing is applied, we see all the metronomes synchronize with each other. We can see this from the Kuramoto order plot (Figure 4.4) that the order reaches 1 and in the phase plot, the phase of all metronomes locks to phase of platform and are anti-phase ratio of π (Figure 4.5).

Chapter 4. Experiments

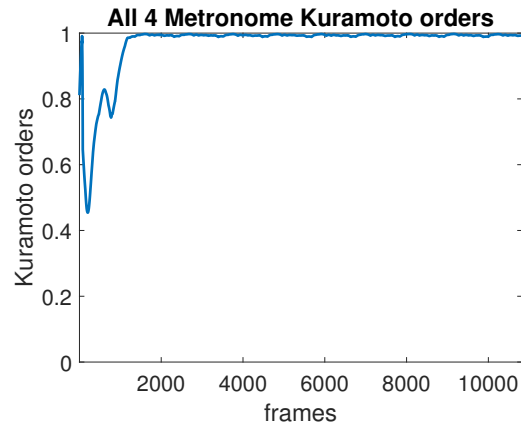


Figure 4.4: Kuramoto order at Higher amplitude(0.3)

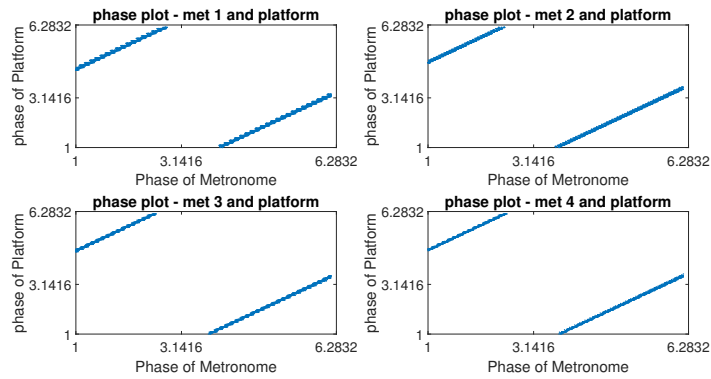


Figure 4.5: Phase plot at 0.3 amp forcing

We check the Kuramoto order for different amplitude from 0.1 to 0.4 and conclude that at least 0.25 amplitude of forcing is required for all the four metronomes to synchronize (Figure 4.6).

Chapter 4. Experiments

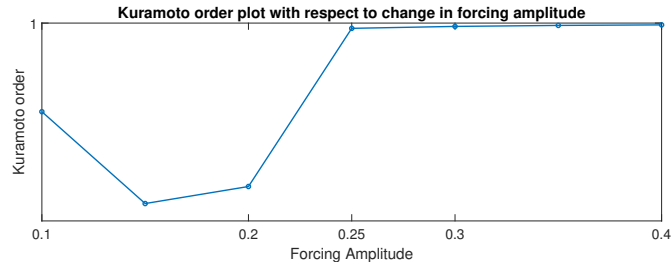


Figure 4.6: Kuramoto order variation with change in amplitude

4.1.2 Driver frequency is different than Metronome frequency

We drive our system of four metronome on the platform with a frequency different than the frequency of the metronome. We varied our driving frequency at: 72BPM, 84BPM, 96BPM, 108BPM, 120BPM, 132BPM, 144BPM, 156BPM and change our driving amplitude at: 0.2, 0.25, 0.3, 0.35 and 0.4.

When the driving frequency is different than the metronomes frequency the Kuramoto order (Figure 4.7) changes with respect to the time and doesn't settle to a value. To determine the kuramoto order we take the average of order over time once the transient is gone.

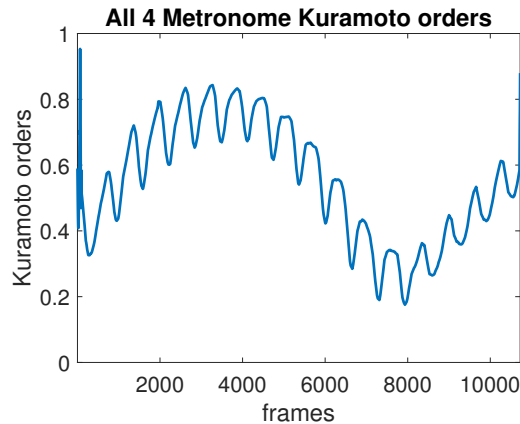


Figure 4.7: Kuramoto order at 0.2 amplitude and 132BPM forcing

Chapter 4. Experiments

We can also see that in the phase plot (Figure 4.8) there is no phase locking between the phase of metronomes and the phase of the platform. Therefore we can say that the metronomes don't synchronize with each other.

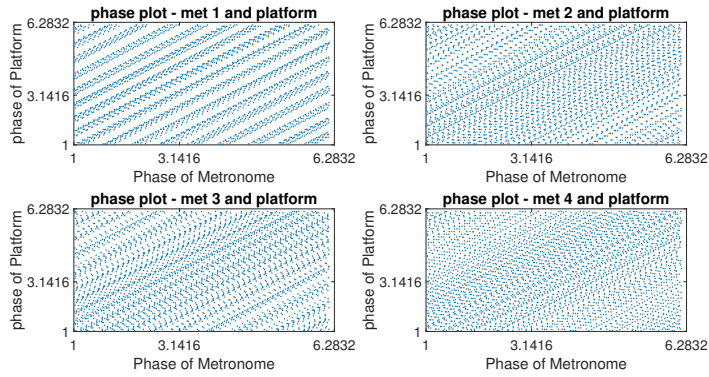


Figure 4.8: Phase plot at 0.2 amp 132BPM forcing

We compute the Kuramoto order for different amplitudes and frequency of forcing and plot the Kuramoto order with respect to a variation in the driving frequency and amplitude (Figure 4.9). We can see in this plot region where Kuramoto order is near one, metronomes synchronize with each other.

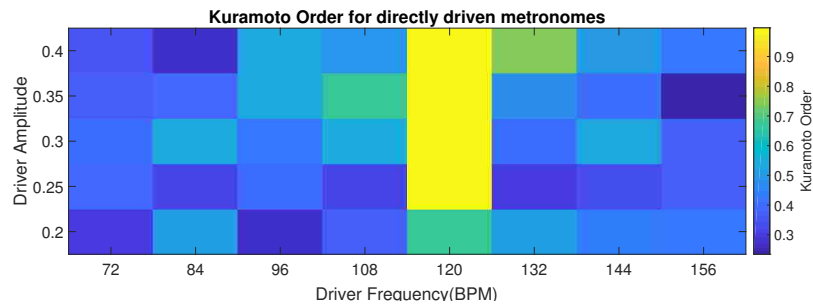


Figure 4.9: Kuramoto order variation with change in driver frequency and amplitude

4.1.3 Metronome frequency and driver frequency are varied while keeping amplitude constant

Here we have four metronomes on a directly driven platform (Figure 4.1). We change the metronomes frequency and the driver frequency to compare how metronomes synchronize with each other. We keep the driver forcing amplitude (0.35) high enough to synchronize (From Figure 4.6). To compare the synchronization we compute the average Kuramoto order [9] after the transient.

We observe that when the driver frequency is equal to the metronome frequency, the Kuramoto order is near to unity (Figure 4.10).

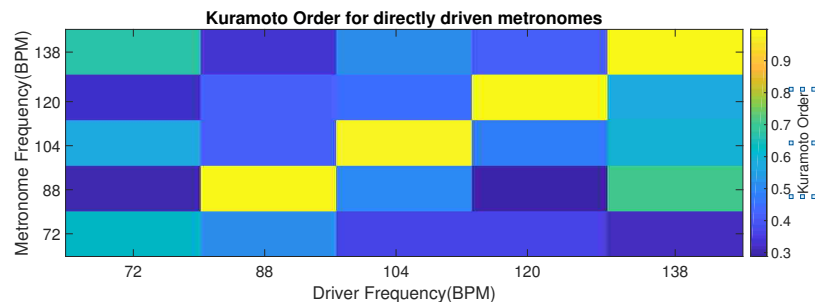


Figure 4.10: Kuramoto order variation with a change in the driver frequency and the metronome frequency

4.1.4 Synchronization in metronomes when non-sinusoidal driving force is applied

Four metronomes are on the platform directly driven with the servo motor with natural frequency of 120BPM. When the driver signal is square waveform with frequency different (96BPM) than metronome frequency we see the Kuramoto order (Figure 4.11) varies and doesn't settle to unity. When the driver frequency (120BPM) is similar to the metronome frequency the Kuramoto order (Figure 4.12) reaches unity.

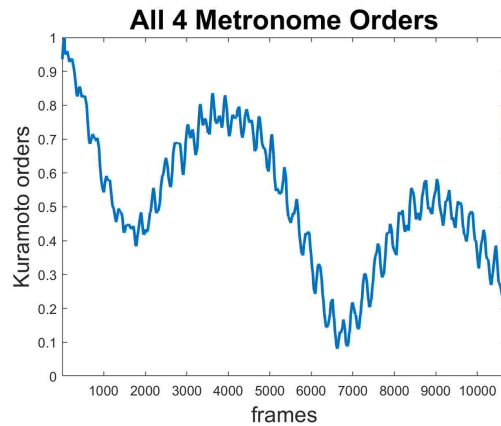


Figure 4.11: Driver square waveform with frequency different then metronomes

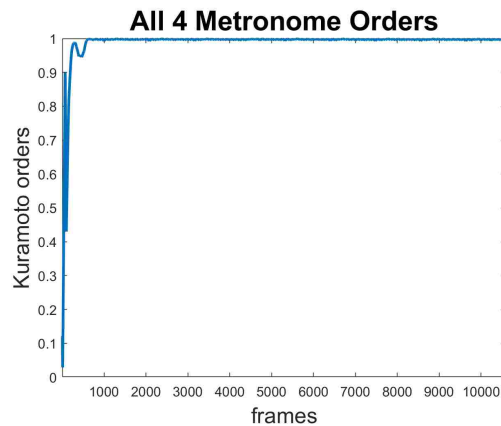


Figure 4.12: Driver square waveform with frequency same as metronomes

When the driver signal is a triangle waveform with a frequency different (96BPM) than the metronome frequency we see the Kuramoto order (Figure 4.13) varies and doesn't settle to unity. When the driver frequency is similar to the metronome frequency the Kuramoto order (Figure 4.14) reaches unity.

Chapter 4. Experiments

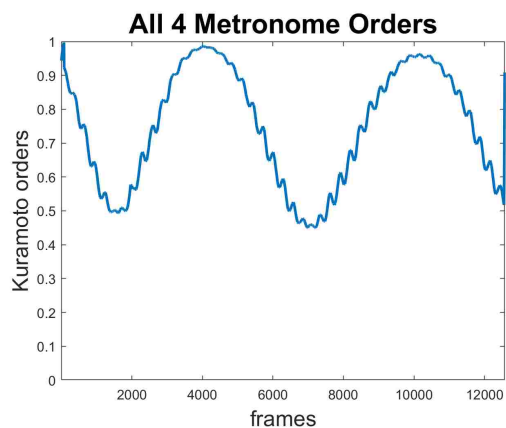


Figure 4.13: Driver triangle waveform with frequency different then metronomes

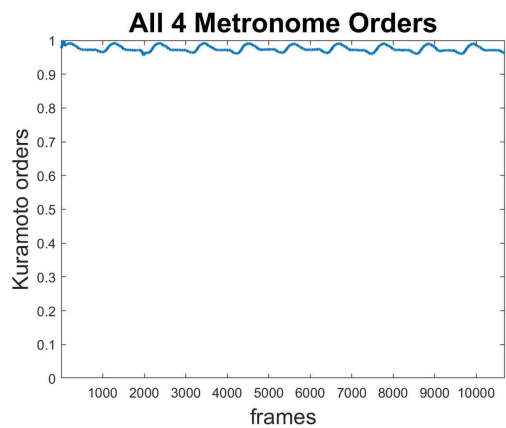


Figure 4.14: Driver triangle waveform with frequency same as metronomes

4.2 Metronomes on platform indirectly driven by servo indirectly

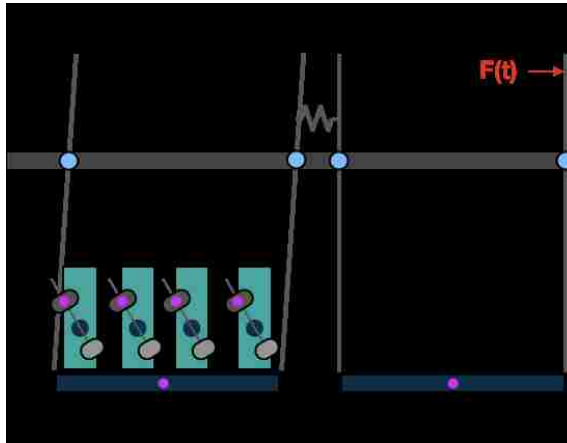


Figure 4.15: Indirect forcing applied on metronomes.

Here the metronomes are on the platform which is driven by forcing on the adjacent platform. The forcing is communicated via spring, therefore metronomes talk to each other too.

4.2.1 Driver frequency equal to Metronome frequency

When the forcing frequency is same as the metronome frequency(120 BPM), we see from figure 4.16 that the metronome synchronize with each other as their Kuramoto order reaches unity.

Also all the phases of all the metronomes locks with the phase of platform with ratio π (Figure 4.17).

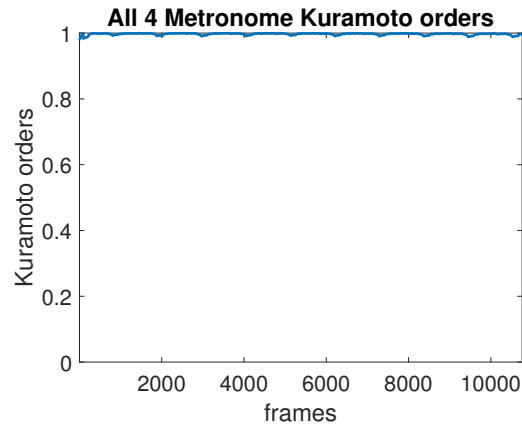


Figure 4.16: Order when forcing is indirect of 0.25 amplitude and 120BPM

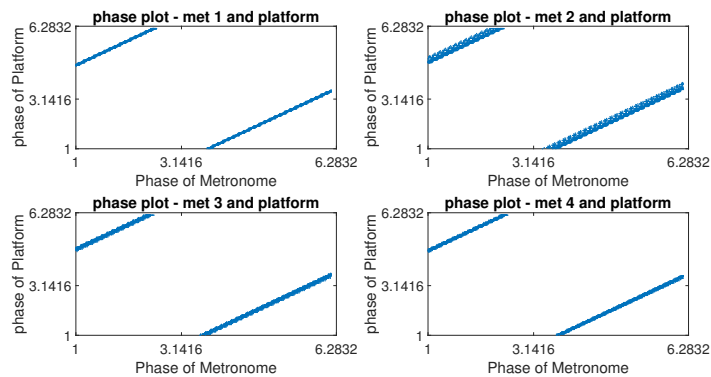


Figure 4.17: Phase of metronome with respect to phase of Metronomes when forcing is indirect of 0.25 amplitude and 120BPM

4.2.2 Driver frequency is different then Metronome frequency

When the driving frequency is different(144BPM) than the metronome frequency, we see the Kuramoto order (Figure 4.18) changes with time and never settles to unity. The metronomes are not synchronized and also their phases never lock to the phase of platform (Figure 4.19).

Chapter 4. Experiments

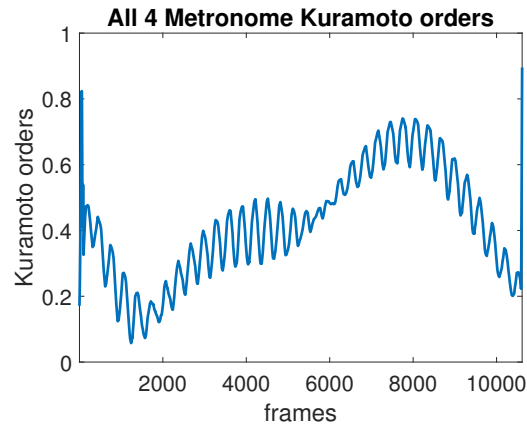


Figure 4.18: Kuramoto order plot of indirectly driven metronomes with 0.2 Amplitude, 144BPM forcing

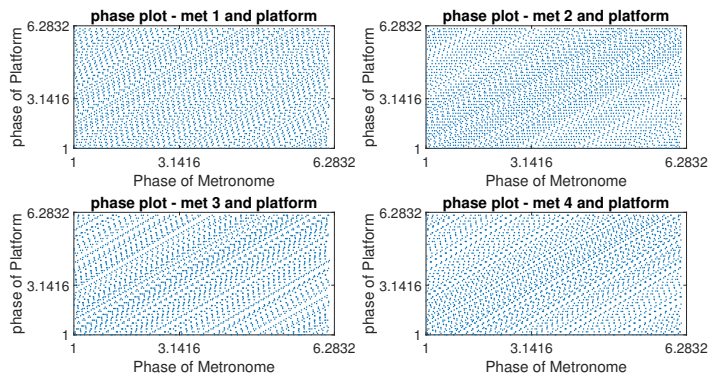


Figure 4.19: Phase plot of indirectly driven metronomes with 0.2 Amplitude, 144BPM forcing

We change the forcing amplitude and frequency and plot the change in kuramoto order (Figure 4.20.)

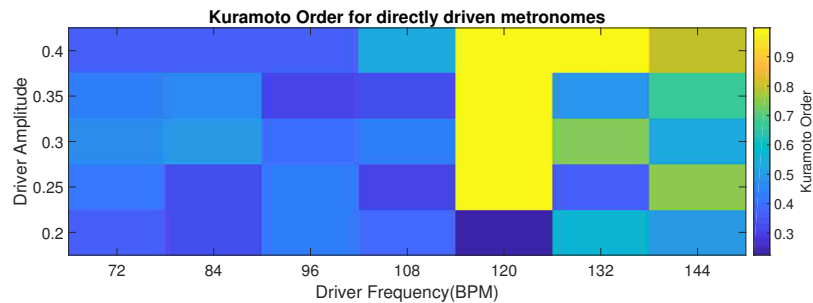


Figure 4.20: Kuramoto order variation with the change in forcing amplitude and frequency.

4.3 Metronomes on platform directly and indirectly driven simultaneously

We set the metronomes on a directly driven and indirectly driven platform at different frequencies. Now we drive our system with a frequency equal to the metronomes on driven platform and then the frequency equal to the metronomes on indirectly driven platform and compare the synchronization.

Metronomes on the driven platform are kept at 120BPM and metronomes on the indirectly driven platform are kept at 80BPM.

When forcing of the frequency same as directly driven platform (120BPM) is given, we observe that the metronome on the directly driven platform synchronize (Kuramoto order reaches 1) and those on the indirectly driven platform do not synchronize (Figure 4.21).

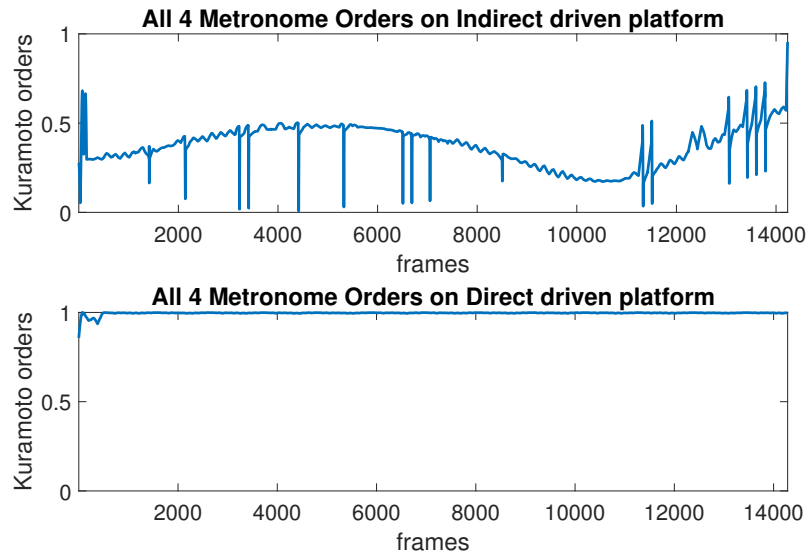


Figure 4.21: Kuramoto order of directly and indirectly driven metronomes when driver frequency is same as metronomes on directly driven platform

When forcing of frequency same as indirectly driven platform (80BPM) is given, we observe that the metronome on the indirectly driven platform synchronize (Kuramoto order reaches 1) while those on the directly driven platform do not synchronize (Figure 4.22).

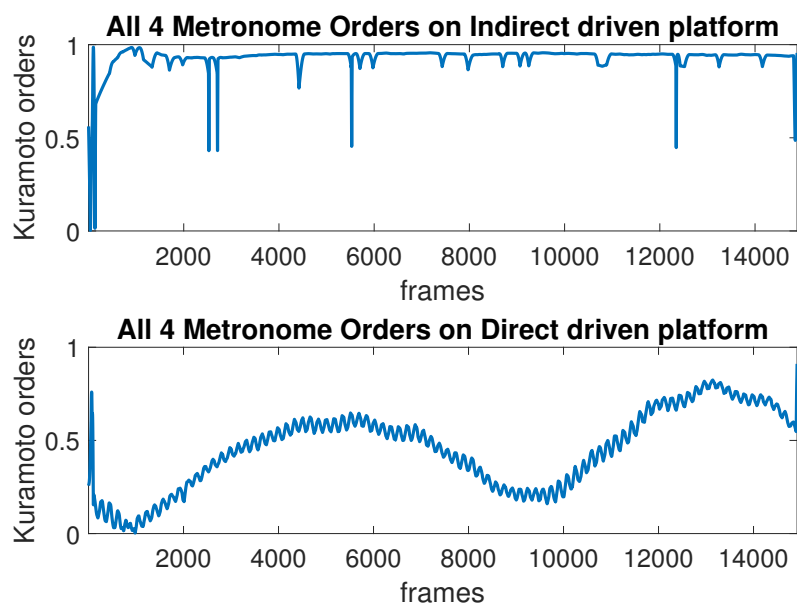


Figure 4.22: Kuramoto order of directly and indirectly driven metronomes when driver frequency is same as metronomes on indirectly driven platform.

Chapter 5

Conclusion & Future work

5.1 Conclusion

- When the driving frequency is same as the metronome frequency, the metronomes on the driven and undriven platforms synchronize. Although, the time taken by them for synchronization varies with the amplitude of forcing.
- When the driving frequency is different than the metronome frequency, the metronomes do not synchronize. Even though some of them synchronize for short period of time, but if we run experiment for a longer period of time, they tend to lose the synchronization with each other.
- Also when the metronomes on the directly and indirectly driven platforms are set to different frequencies with external driving, we see that only the metronomes whose frequency matches the frequency of the driver are synchronized.
- Metronomes tend to synchronize more when the forcing is given to them indirectly (via spring). This way they get the forcing from the servo and can talk

to each other too.

5.2 Future work

- We plan to conduct more experiments where we look at how the metronomes react to the driver on a platform with different frequencies.
- We have a new camera system from Basler which would allow us in future to expand this system by looking at more number of metronomes where the driving is given through feedback.

References

- [1] Daniel M Abrams, Rennie Mirollo, Steven H Strogatz, and Daniel A Wiley. Solvable model for chimera states of coupled oscillators. *Physical review letters*, 101(8):084103, 2008.
- [2] DM Abrams. Dm abrams and sh strogatz, *phys. rev. lett.* 93, 174102 (2004). *Phys. Rev. Lett.*, 93:174102, 2004.
- [3] Karen Blaha, Ryan J Burrus, Jorge L Orozco-Mora, Elvia Ruiz-Beltrán, Abu B Siddique, VD Hatamipour, and Francesco Sorrentino. Symmetry effects on naturally arising chimera states in mechanical oscillator networks. *Chaos: An Interdisciplinary Journal of Nonlinear Science*, 26(11):116307, 2016.
- [4] John Buck and Elisabeth Buck. Mechanism of rhythmic synchronous flashing of fireflies: Fireflies of southeast asia may use anticipatory time-measuring in synchronizing their flashing. *Science*, 159(3821):1319–1327, 1968.
- [5] Sune Danø, Preben Graae Sørensen, and Finn Hynne. Sustained oscillations in living cells. *Nature*, 402(6759):320, 1999.
- [6] C Huygens. Lhorlogea pendule. *Oeuvres complètes de Christiaan Huygens*, 17, 1967.
- [7] IZ Kiss. Iz kiss, y. zhai, and jl hudson, *science* 296, 1676 (2002). *Science*, 296:1676, 2002.
- [8] Minayori Kumamoto, Toru Oshima, and Tomohisa Yamamoto. Control properties induced by the existence of antagonistic pairs of bi-articular musclemechanical engineering model analyses. *Human Movement Science*, 13(5):611–634, 1994.
- [9] Yoshiaki Kuramoto and Dorjsuren Battogtokh. Coexistence of coherence and incoherence in nonlocally coupled phase oscillators. *arXiv preprint cond-mat/0210694*, 2002.

References

- [10] Chen Liu, David R Weaver, Steven H Strogatz, and Steven M Reppert. Cellular construction of a circadian clock: period determination in the suprachiasmatic nuclei. *Cell*, 91(6):855–860, 1997.
- [11] Erik A Martens. Chimeras in a network of three oscillator populations with varying network topology. *Chaos: An Interdisciplinary Journal of Nonlinear Science*, 20(4):043122, 2010.
- [12] Erik Andreas Martens, Shashi Thutupalli, Antoine Fourrière, and Oskar Hallatschek. Chimera states in mechanical oscillator networks. *Proceedings of the National Academy of Sciences*, 110(26):10563–10567, 2013.
- [13] Thomas M Massie, Bernd Blasius, Guntram Weithoff, Ursula Gaedke, and Gregor F Fussmann. Cycles, phase synchronization, and entrainment in single-species phytoplankton populations. *Proceedings of the National Academy of Sciences*, page 200908725, 2010.
- [14] Donald C Michaels, Edward P Matyas, and Jose Jalife. Mechanisms of sinoatrial pacemaker synchronization: a new hypothesis. *Circulation Research*, 61(5):704–714, 1987.
- [15] Mark J Panaggio and Daniel M Abrams. Chimera states: coexistence of coherence and incoherence in networks of coupled oscillators. *Nonlinearity*, 28(3):R67, 2015.
- [16] H.J.; Vilkkko M.K. Pyrhonen, V.-P.; Koivisto. A reduced-order two-degree-of-freedom composite nonlinear feedback control for a rotary dc servo motor. In *2017 IEEE 56th Annual Conference on Decision and Control (CDC)*. IEEE, 2017.
- [17] Steven H Strogatz, Daniel M Abrams, Allan McRobie, Bruno Eckhardt, and Edward Ott. Theoretical mechanics: Crowd synchrony on the millennium bridge. *Nature*, 438(7064):43, 2005.
- [18] Annette F Taylor, Mark R Tinsley, Fang Wang, Zhaoyang Huang, and Kenneth Showalter. Dynamical quorum sensing and synchronization in large populations of chemical oscillators. *Science*, 323(5914):614–617, 2009.
- [19] Kurt Wiesenfeld, Pere Colet, and Steven H Strogatz. Frequency locking in josephson arrays: Connection with the kuramoto model. *Physical Review E*, 57(2):1563, 1998.
- [20] Anna Wirz-Justice. Biological rhythm disturbances in mood disorders. *International Clinical Psychopharmacology*, 21:S11–S15, 2006.

References

- [21] Mark J Zylka, Lauren P Shearman, David R Weaver, and Steven M Reppert. Three period homologs in mammals: differential light responses in the suprachiasmatic circadian clock and oscillating transcripts outside of brain. *Neuron*, 20(6):1103–1110, 1998.